

## Artificial Neural Network Modelling and Simulation for Gas Leak Detector Performance in Geregu Gas Turbine Power Plant

Nasir Muhammad Lawal<sup>1</sup>, Abubakar Kandi Mohammed<sup>2</sup> and Idris Ibrahim Ozigis<sup>1</sup>

<sup>1</sup>Department of Mechanical Engineering, University of Abuja FCT Abuja, Nigeria

<sup>2</sup>Geregu power plc. Ajaokuta, Kogi state.

Email: [nasir.lawal@uniabuja.edu.ng](mailto:nasir.lawal@uniabuja.edu.ng) / [idris.ozigi@uniabuja.edu.ng](mailto:idris.ozigi@uniabuja.edu.ng) / [abubakarkandi@yahoo.com](mailto:abubakarkandi@yahoo.com)\*

### Article Info

**Keywords:** Artificial neural network, Calibrators, Gas leak detectors, Geregu gas turbine, Harmattan.

Received 26 May 2024

Revised 28 June 2024

Accepted 26 August 2024

Available online 15 sept. 24

<https://doi.org/10.5281/zenodo.13765392>

ISSN-2682-5821/© 2024 NIPES Pub. All rights reserved.

### Abstract

*This study is aimed at reducing false alarms in Geregu gas power plant by integrating an Artificial Neural Network (ANN) with the conventional calibrated detectors to improve their performance. The impact of industrial gas leakage to human and environment has necessitated the use of detectors to monitor their presence and concentration. However, the inability of the detectors to differentiate actual gas leaks from unanimous gas figments results to false alarms. Primary causes of false alarms were identified with ambient seasonal factors and human errors as leading indicators among others. An ANN with five inputs, two hidden layers of six and two neurons with an output was developed, trained and validated using the plants historical alarm data from 2019 to 2024. The results obtained shows false alarms occurred almost 100% in January and December which indicates the great influence of ambient condition during harmattan periods. Slight traces of human operation error were also observed. With an epoch of 65, the ANN produced an almost 92.2% output matching with a mean absolute error (MAE) of 0.371, root mean square error (RMSE) of 0.304 and R<sup>2</sup> representation of 87%. The model thus, demonstrate the effectiveness of gas detectors integrating with artificial intelligence (AI) to predict true gas leak from unanimous causes of false alarm. The ANN, however, cannot completely take the place of conventional calibrators, but will improve the overall system performance.*

### 1.0. Introduction

Gas leakage in industries, public or residential premises is one of the sources of harmful air pollution and climatic degradation. It creates emission hotspots, significant public human health impacts and environmental issues. Carter [1], gave an example, the effects of methane leakage, which is a very potent greenhouse gas, was estimated to be more than 80 times the warming potential of CO<sub>2</sub> over a twenty year period. This is partly due to none established standard systems for estimation of the quantity of gas leakage to the immediate environment. Climate Nexus [2], presents a life cycle gas leakage rate for 71 cities in United States – US, and it shows that a huge gap exists between annual reports and the true values of leakage, which were determined to be four folds higher in some cases. This claim has a very serious concern as CO<sub>2</sub> is responsible for 60% of the greenhouse effect, and four times that value is a huge escalation. Honeywell [3] reported an example that more fatality is recorded from gas exposure from leakage, compared to that from explosions. Tabuchi [4] and Climate Nexus [2] asserted that at a global level, it takes as small as 0.2% of obnoxious gas leakage to produce a global impact as high as the effect from the use of coal in stoker combustion without retrofitted flue gas control. Most gas leak rates are measured with flow meter having an accuracy of about  $\pm 2\%$ . Compared to Climate Nexus and Hiroko's assertions, such instrument will lead to about

10 times of actual leak than indicated. This is why routine monitoring of gas leakage in the plant is compulsory to prevent severe injuries, fatalities and significant damage to property as mentioned by Oloche et al., [5].

In many industrial establishments, gas leakage is monitored using gas detectors. Honeywell [3] listed the typical sectors that require gas detection to include industrial processes involving the use of and manufacture of highly dangerous substances particularly toxic and combustible gases, petrochemical industries and thermo-fluid plants especially in electricity generation plants. In power generation plants, gas detectors are mounted around turbine bearing seals and housings, boilers and burners. Gas detectors are devices that sense the presence of gases in an area often as part of a safety system. Their capabilities often include detection of combustible, flammable and toxic gases and oxygen depletion in built environments, where an early level of gas detection from 0% up to lower explosive limits are set to initiate alarms and activate shut down procedure [6, 7, 8]. Common available gas leak detectors include Infra-red point sensors, Ultra-sonic detectors, Electro-chemical gas sensors and semi-conductor sensors [7, 8, 9].

In operation, Infra-red imaging detectors scan a laser across field of view and look for back scattered light at the absorption line depending on the wavelength of a specific target gas, Muda [10]. The ultra-sonic detectors use the acoustic emission created when pressured gas expands in low pressure area through a small orifice. On the other hand, electro-chemical detectors use the principles of gas diffusion through porous membrane to an electrode where it is chemically oxidized or reduced, [8, 9, 10]. Gas detection systems are extremely important in power plants because of the need for continuous monitoring without human presence. The adoption of fixed-point gas detectors is the best fit for such applications like in gas turbine engine for electricity generation power plants, [7, 9, 11, 12, 13].

Infra-red gas detectors are one of the most widely used fixed-point detectors for gas turbine applications, [7, 14, 15]. [7, 12, 13] outlined the qualities of Infra-red detectors that make them attractive for power gas turbine applications to include fast response time, ability to work in inert atmosphere and ability to detect several gases. [16 - 19] reported that sensors and detectors tend to drift when exposed to high concentration of gases and vapour, or extreme conditions such as high/low humidity with mass concentration of air borne particles. Such extreme conditions are prevalent in vicinities where gas turbine detectors are commonly mounted in power generation companies. To improve the sensitivity of detectors, regular calibration is required especially for flammable and combustible gases to ensure the accuracy, reliability and functionality of the gas detectors, [20, 21, 22]. The overall performance of a gas turbine is also linked with the proper performance of gas detectors in operation mostly achieved through regular calibrations, [23, 24, 25]. The calibration of gas detectors conventionally requires the use of a standardized known concentration test gas for a particular brand and type of detector, [3, 26, 27].

Failure to detect and quantify gas leaks in power plant industries like gas turbines for power generation is disastrous. However, false alarms of gas leak could lead to plant shutdowns, emotional destabilization and overall reduction in productivity. Though different types of gas leak detectors are used to protect people, equipment, immediate environment with negligible errors, the need to predict and mitigate false alarm has become a productivity dependent factor that must be reduced if not completely eradicated. The sensors lack means of discerning some leak gases features from the figments of similar environmental conditions in the vicinity of power plants. This gap can be filled using artificial neural network – ANN comparator, as elaborated by [28, 29] to differentiate false gas situation from real leak features in order to minimize the occurrence of false alarms and their

attendant effects. The significance of integrating an ANN comparator with the current detectors is to improve system reliability and plant productivity through the establishment of actual maintenance and calibration frequencies.

## 2.0 Material and Method

### 2.1 Materials

**2.1.1 Geregu Gas Power Plant System** was used for the study. The main components that are susceptible to gas leak in the plant are:

**i. Gas storage** facility receives and stores natural gas momentarily to allow for steady and continuous gas supply. Two infrared detectors are mounted for quick leak detection.

**ii. Fuel Combustion Chamber ports:** The fuel gas system comprises of dual arms with turbo-annular combustion chambers - left and right. On each arm is mounted two infra-red type gas detectors.

**iii. The fuel gas skid:** this is a fuel gas conditioning system that screen solid and liquid content from getting into the combustion chamber and provides the required thermodynamic state that is suitable for the downstream equipment and emission criteria.

**iv. Combustion Chamber Exhaust:** like every other exhaust, it serves as the passage for combusted gas to escape the combustion chamber. In the event of incomplete combustion, which is always the case with several degree of efficiency, CO, CO<sub>2</sub>, hydrocarbons and particulate matters are released.

**2.1.2 Instrumentation:** The gas turbine instrumentations that are applicable to gas leak detection include:

**i. Gas detectors:** these are devices that sense the presence of gases in an area which may be in a closed or open built environment within a gas power plant. The infrared detectors installed in Geregu power plants have the following specifications: 3.0 watts transmitter relay module with nominal voltage range of 18-30 vdc with an output signal current from the transmitter is in the range of 4 to 20 mA, [3].

In each location stated earlier, two gas detectors are installed with their sensors connected to potable calibrators via a cable network from a junction box as shown Figure 1.

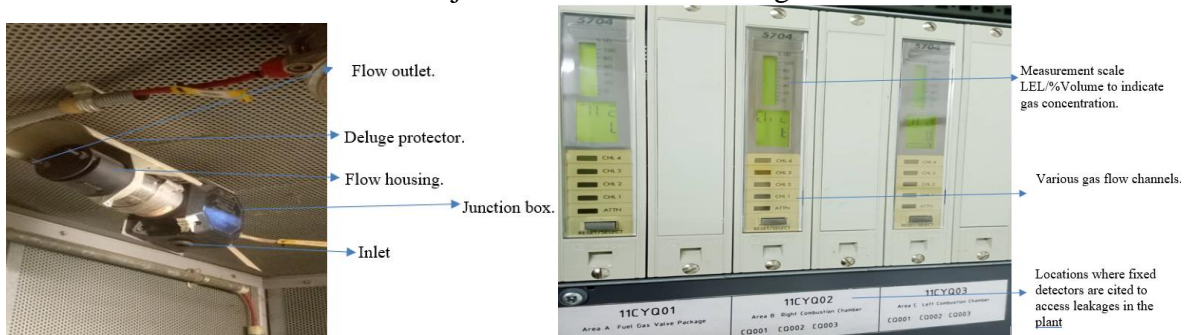


Figure 1: Infrared Detectors used in Geregu Power Plants  
(a) Fixed detector in place. (b) Detector panels with location numbering.

**ii. The gas detection panel:** It receives output signal from the transmitter of the gas detector sensor. On the panel is screen indicator from which detector gas leakage alarm source can be accessed. Typical panel installed in Geregu power plant is shown in Figure 1b.

**iii. Gas detector calibrator:** A potable Zellweger analytic type of calibrator is used in Geregu power plant with operating temperature of -40 to 40°C [3, 30], 0 to 50% lower explosive limit (LEL), with a resolution of 1% (1 ppm), detectable range of 0 to 500 ppm and response time of less than

10 to 12.3 seconds for gases like Methane, Carbon Monoxide, Hydrogen Sulphide and Sulphur dioxide, [3, 30, 31].

**2.1.3 Working Fluid:** the main working fluids are:

- i. **Air:** with an approximate density of  $1.25\text{kg/m}^3$ , [32, 33] specific heat capacity of  $1.005\text{kJ/kg-k}$  [34] and dynamic viscosity of  $1.802 \times 10^{-5} \text{ kg/m-s}$  at ISO [35].
- ii. **Natural gas:** predominantly Methane and others [25, 26].
- iii. Combusted gases which include  $\text{CO}_2$ ,  $\text{CO}$ ,  $\text{HC}$ ,  $\text{PM}$  and other minor gases.

**2.2 Methods**

The General procedure used for improving the gas detector sensitivity using ANN based approach is similar to ones used by [36 - 39] is shown in Figure 2.

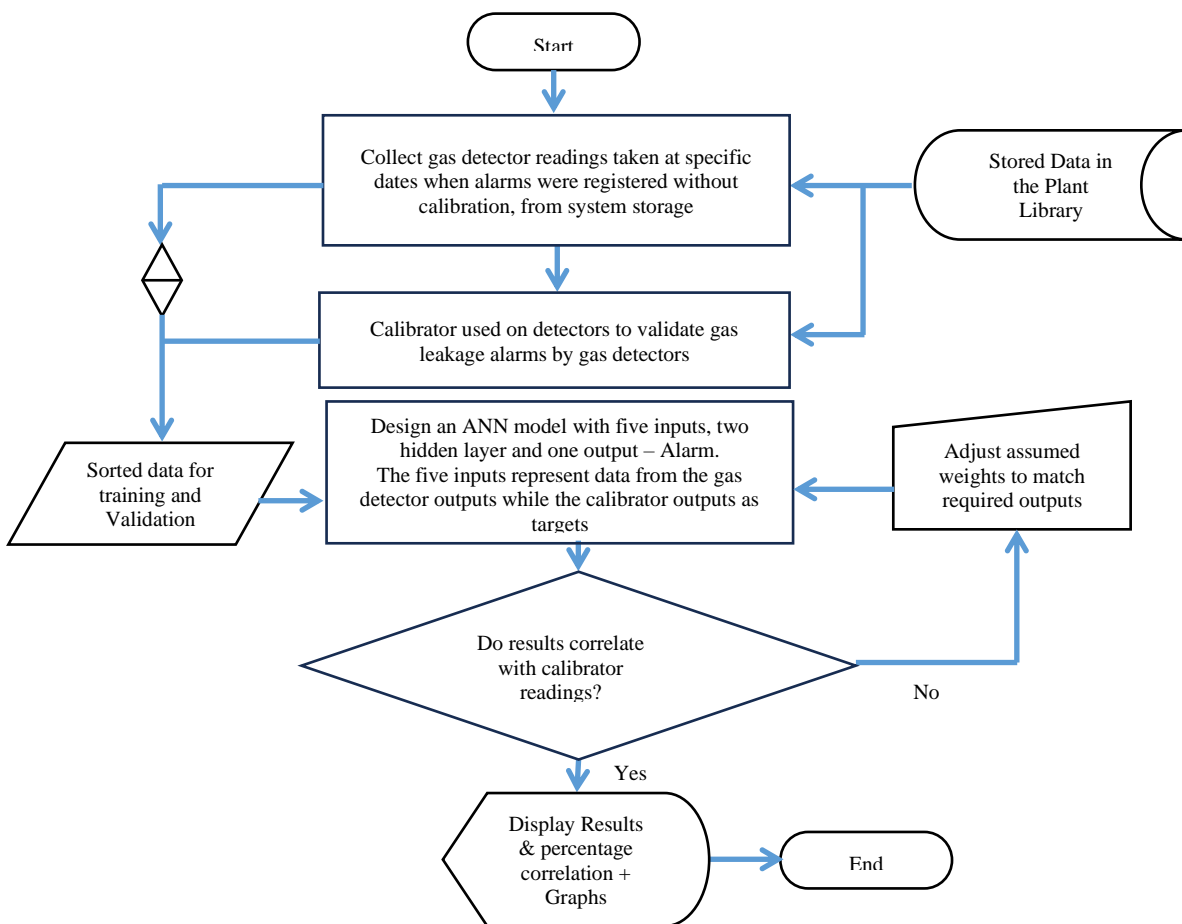


Figure 2: Flow chat for ANN based gas leak

**2.2.1 Data Set Collection and Model Formulation**

Technique followed similar pattern used by [37, 40, 41, 42, 43]. Data set for 6 years were used; from around January 2019 to early 2024. Some of the gas leakage alarm samples captured by the gas detectors with the respective dates as obtained from the HMI - control panel where large historical data is archived is shown in Table 1.

Table 1: Alarm trigger sample - Possible input for actual and calibrators targeted outputs

Date	x1	x2	x3	x4	x5	Output	Calibrated
01/01/2019	1	1	0	0	1	1	0
04/04/2019	0	0	1	1	1	1	1
08/07/2019	0	0	1	0	1	0	1
18/01/2020	0	1	0	0	1	1	1
13/11/2020	1	1	1	0	0	0	1
15/12/2020	1	1	0	1	0	1	1
21/01/2021	1	1	0	0	1	0	1
25/01/2021	1	0	0	1	1	0	1
27/05/2023	0	0	1	1	1	1	1
17/08/2023	0	1	1	1	0	1	1
05/01/2024	0	1	0	1	1	1	1
06/01/2024	0	1	1	0	1	1	0
22/01/2024	1	0	1	0	1	0	1

Table 1 shows the alarms that triggered during five years period, approximately three times per year. In the first column, '1' indicates alarm without any indication of whether it is real or false. In the second column, calibrators are used and the results indicate '1' for true alarm and '0' for false alarm. The ANN model was designed using data from actual gas detector and the calibrator. Out of 18 events captured by the gas detector, 72% case scenarios were used for training and the rest for validation.

### 2.2.2 The design concept

The concept is based on the combination of the history of the factors that could influence alarm due to gas detection which may be true and false as depicted in Figure 3.

### 2.2.3 Design Architecture of the Artificial Neural Network

The alarm from an infra-red detector may come from equipment health condition (x1), location distance of the detectors (x2), working fluid state equilibrium (x3), immediate ambient condition (x4) and Human operation error (x5). These five factors are considered as the input to the ANN. The representative ANN architecture is given in the neural interconnecting chart shown in Figure 4.

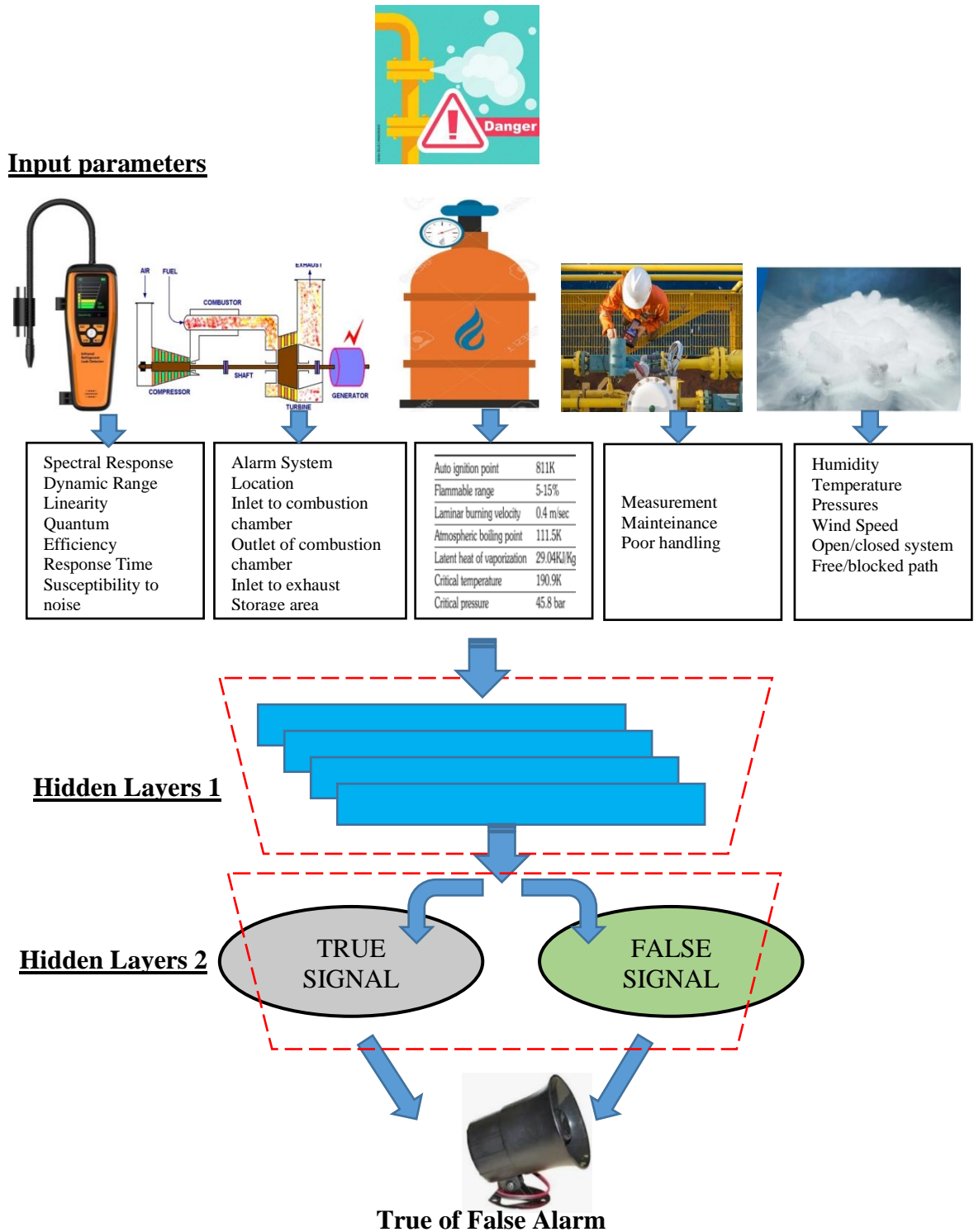


Figure 3: Pictorial of five variable and pre-conditions which prompt gas leak alarms.

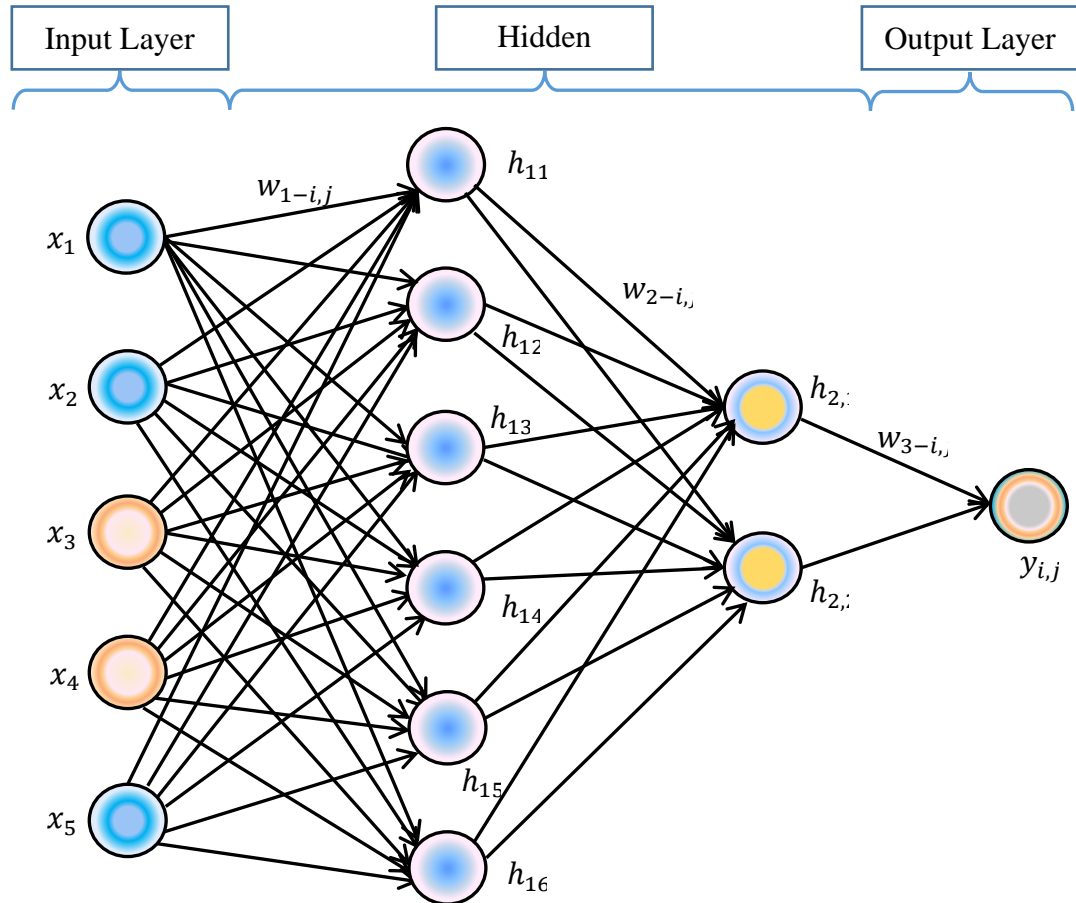


Figure 4: Design Architectural of the Artificial Neural Network

The artificial Neural Network (ANN) for Gas Leak Detector has the following features.

**Inputs:** there are five inputs defined below:  $x_1$  = Equipment fault,  $x_2$  = Detector location,  $x_3$  = Thermo-fluid condition,  $x_4$  = Environmental impact and  $x_5$  = Human error. The values of the data sets for each  $x_i$  are binary with ‘0’ indicating no fault/impact thus classifying the alarm as false, or ‘1’ indicating fault/impact is present, thus producing a real alarm.

**Hidden Layers:** there are two hidden layers; Layer-1 (6 neurons) and Layer-2 (2 neurons).

**Output:** the output represents an alarm which may be real ‘1’ or false ‘0’.

**Activation Functions:** the two activation functions adopted are Sigmoid for hidden layers and linear function for the output layer.

**Training Algorithm:** Combined forward- and backward-propagations training algorithm was used. It is a supervised learning in which binary data sets  $n$  with  $X_i$  input and  $Y_i$  output vectors are given for  $i = 1, 2, \dots, m$  caused of gas leakage and the consequential alarm.

A typical training set for the supervised learning using binary classification 0/1, for  $n = 3$  and  $m = 5$ , is given in Table 2:

Table 2: Supervised training data set sample for Gas leak Detector Model

$x_1$	$x_2$	$x_3$	$x_4$	$x_5$	$y$
1	0	0	1	0	0
0	1	0	0	1	1
1	1	1	0	1	1

## 2.2.4 Model Formulation and Design Codes in MatLab

The features, applied weights and biases are given in MATLAB environment in code 1a:

### **Code 1a: Network Architecture Definition**

```
% Network Architecture Definition
Inputs = 5;
numInputs = size(inputs, 2); % Number of input neurons
numHidden1 = 6; % Number of neurons in the first hidden layer
numHidden2 = 2; % Number of neurons in the second hidden layer
outputs = 1;
numOutputs = size(outputs, 2); % Number of output neurons
% Initialize weights and biases
weights1 = rand(numInputs, numHidden1) - 0.5; % Weights for layer 1
biases1 = rand(1, numHidden1) - 0.5; % Biases for layer 1
weights2 = rand(numHidden1, numHidden2) - 0.5; % Weights for layer 2
biases2 = rand(1, numHidden2) - 0.5; % Biases for layer 2
weights3 = rand(numHidden2, numOutputs) - 0.5; % Weights for output layer
biases3 = rand(1, numOutputs) - 0.5; % Biases for output layer
```

A forward propagation function is then applied to it using the relation in Equation 1:

$$y(z) = \frac{1}{1+e^{-z}} \quad (1)$$

Where  $y$  is a normalization function that constrain the output to stay between 0 and 1, and  $z$  is a transfer-enthalpy function defines as:

$$z = \sum_{i=1}^n x_i w_{i,j} + b_{i,j} \quad (2)$$

Where  $x_i$  is the input variable  $w_{i,j}$  is the weight given to each transfer path and  $b_{i,j}$  is the bias defined as the sum of the product of the input and the assigned weight to the neuron. The MATLAB code-1b presents the implementation of the bias and propagation function.

### **Code 1b**

```
% Forward propagation function
function output = forward_propagation(input, W1, b1, W2, b2, W3, b3)
    z1 = W1 * input + b1;
    a1 = sigmoid(z1);
    z2 = W2 * a1 + b2;
    a2 = sigmoid(z2);
    z3 = W3 * a2 + b3;
    activationFunction = @(x) 1./(1 + exp(-z3));
    output = sigmoid(z3);
end
```

## 2.2.5 The Model Training Codes

After the model and mini-coding, the ANN model was trained with detector's historical data obtained from both calibrator and the actual detector. Nine years data – from 2019 to early 2024 was used for training the model. The codes for training parameters and activation functions are given in code 2a.

### **Code 2a**

```
% Training parameters Parameters
learningRate = 0.1; % Learning rate
epochs = 100; % Number of training epochs
% Training loop
for epoch = 1:epochs
    % Forward propagation
    hidden1 = activationFunction(inputs * weights1 + biases1);
    hidden2 = activationFunction(hidden1 * weights2 + biases2);
    outputsPredicted = activationFunction(hidden2 * weights3 + biases3);
```

**2.2.6 Testing and Validation:** the ANN is applied to a set of data with known outcome, and it mimicked the actual detector by predicting outcomes at some randomly chosen dates (28% of sample) to validate the potency of the model. The results obtained are compared to the known outcome and the difference (error) estimated. A backward propagation signal is implemented to provide signals for adjusting the weights and biases until the outputs are within acceptable close values to the targets.

The sample codes for backward propagation, weight and bias adjustment is given in code 2b

**Code 2b**

```
% Calculate error
error = outputs - outputsPredicted;
% Backpropagation
delta3 = error .* outputsPredicted .* (1 - outputsPredicted);
delta2 = delta3 * weights3' .* hidden2 .* (1 - hidden2);
delta1 = delta2 * weights2' .* hidden1 .* (1 - hidden1);
% Update weights and biases
weights3 = weights3 + learningRate * hidden2' * delta3;
biases3 = biases3 + learningRate * sum(delta3);
weights2 = weights2 + learningRate * hidden1' * delta2;
biases2 = biases2 + learningRate * sum(delta2);
weights1 = weights1 + learningRate * inputs' * delta1;
biases1 = biases1 + learningRate * sum(delta1);
```

**2.3 The performance Evaluation Criteria for The ANN Model**

In this paper, four performance indicators; root mean square error (RMSE), Linear regression (LR) were the criteria utilized to establish the accuracy of the ANN model used for forecasting.

i. **The (RMSE)** is defined as the difference between the predicted and experimental values define as:

$$RMSE = \sqrt{\frac{\sum_{i=1}^m (x_i - o_i)^2}{m}} \tag{3}$$

Where  $x_i$  is the desired output for node p and  $o_i$  is the system output for node i,  $m$  is the sample number. As error measurement criteria, the lower the RMSE the more accurate is the model evaluated.

ii. **Linear Regression:** Kanade [44, 45], defined Linear Regression as an algorithm which provides linear relationship between independent and dependent variables. The linear correlation between the two variable vectors  $x_i$  and  $y_i$  is defined as:

$$r = \frac{n \sum_{i=1}^n x_i y_i - (\sum_{i=1}^n x_i) (\sum_{i=1}^n y_i)}{[n \sum_{i=1}^n x_i^2 - (\sum_{i=1}^n x_i)^2][n \sum_{i=1}^n y_i^2 - (\sum_{i=1}^n y_i)^2]} \tag{4}$$

Finding out the linear correlation before fitting a model is a useful tool in identifying the kind of relationships between the vectors, as well as level of accuracy associated to the group of data set used. The level of accuracy is influenced by the percentage of input data sets that nominally accounts for variation in the output. This factor is termed the coefficient of determination,  $R^2$ , defined as [xxx]:

$$R^2 = \frac{\sum_{i=1}^n (\hat{y}_i - \bar{y})^2}{\sum_{i=1}^n (y_i - \hat{y}_i)^2} \tag{5}$$

Where  $R^2$  is the coefficient of determination,  $n$  is the number of data sets,  $y_i$  is the actual data value,  $\hat{y}_i$  is the regression value and  $\bar{y}$  is the mean value of the actual data.

iii. **Cross-Entropy:** For binary classification, Maximum Likelihood Estimator (MLE) is also used to determine the cumulative loss between target values and actual ANN outputs. MLE for  $n$  data sets is defined as [xxx]:

$$MLE = \text{Maximize: } \prod_{i=1}^n q(X_i)^{y_i} [1 - q(X_i)^{1-y_i}] \tag{6}$$

Log was Applied to Equation (6), the cross-entropy cost function CE, defined as [xxx]:

$$CE = \sum_{i=1}^n [-y_i \log(q(X_i)) - (1 - y_i) \log(1 - q(X_i))] \quad (7)$$

The cost function, is defines the cumulative loss in binary classification training.

**iv.** Percentage of good classification (PGC): is simply defined as the average of ANN output in percentage. It is calculated from [xxx]:

$$\frac{1}{n} \sum_{i=1}^n y_i \quad (8)$$

It gives a quick initial judgement of closeness of targeted and actual outputs.

The MatLab Codes for the Model Performance evaluation covers the four statistical measures of accuracy and dispersion, namely: RMSE, Cross-entropy, linear correlation and PCG.

**Code 3a**

```
% Calculate performance metrics
rmse = sqrt(mean(error.^2));
r = corr(outputs, outputsPredicted);
rSquared = r^2;
crossEntropy = -mean(outputs .* log(outputsPredicted) + (1 - outputs) ...
    .* log(1 - outputsPredicted));
pcg = sum(outputsPredicted >= 0.5 & outputs == 1) / sum(outputs == 1);
% Display progress
if mod(epoch, 100) == 0
    disp(['Epoch:', num2str(epoch), ', RMSE:', num2str(rmse), ', R^2: ', ...
        num2str(rSquared), ', Cross Entropy: ', num2str(crossEntropy), ...
        ', PCG:', num2str(pcg)]);
end
end
```

To generate loss analysis, some sample data for demonstration purposes were used and the codes for generating the graphs are in code 3b.

**code 3b**

```
% Performance curves presentation with a set of separate test dataset
figure;
subplot(2, 2, 1);
plot(1:epochs, rmse);
title('RMSE vs Epochs');
xlabel('Epochs');
ylabel('RMSE');

subplot(2, 2, 2);
plot(1:epochs, rSquared);
title('R^2 vs Epochs');
xlabel('Epochs');
ylabel('R^2');

subplot(2, 2, 3);
plot(1:epochs, crossEntropy);
title('Cross Entropy vs Epochs');
xlabel('Epochs');
ylabel('Cross Entropy');

subplot(2, 2, 4);
plot(1:epochs, pcg);
title('PCG vs Epochs');
xlabel('Epochs');
ylabel('PCG');

title('ANN Performance Curves');
```

### 3.0 RESULT AND DISCUSSION

The model was built and trained with 72% of the data from the actual detector and calibrator measurements archived from 2015 to 2024. Randomly selected data from the remaining 28% mainly from 2019 and 2024 were used test run the model. Similarly, Table 2 contains sample set used for testing the validity of the ANN model while Table 3 contains comparative performances of the actual detector, calibrator and the ANN modelled gas detector sensor. Figure 7 is the chart showing gas leak sensitivity ratios for the 18 cases recorded between 2019 and 2024 for the gas detector and the calibrator.

#### 3.1 Data Classification and Alarm Representation

The data used is classified into two non-calibrated and calibrated data, each of which presents two possible outcomes – true or false alarm on combination of some factors that are responsible to actuate the detector measurement and hence, trigger the alarm.

The bar-chart in Figure 5 shows the frequency of true or false from the sample readings of the actual detector and that of the calibrator.

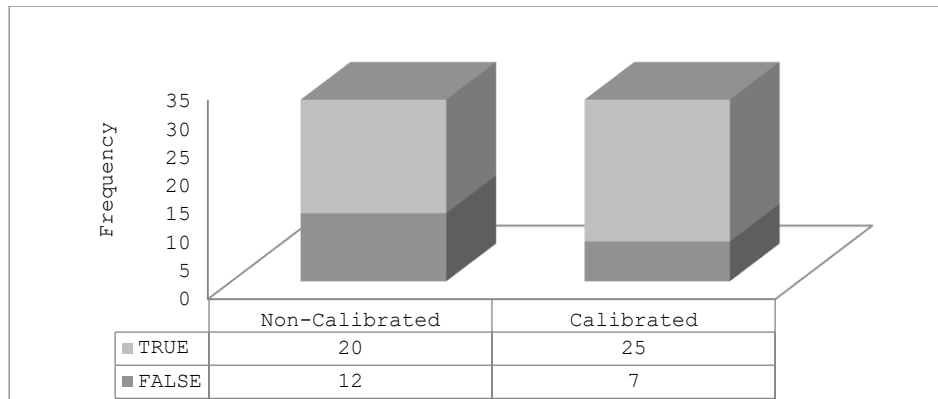


Figure 5: Percentage detector and calibrator Alarms for 18 cases recorded between 2019-2024  
The total binary data (0, 1) is 64; 32 for calibrated and non-calibrated each. In non-calibrated, 20 are true '1' representing 63% and 12 are false '0' representing 37%. After the detector is calibrated, 25 are true alarm '1' representing 78% while 7 of them represents false '0' representing 22%.

Detector faults may be due to several issues; however, all of them result to sensor drifting and possible false alarm. This was generally classified as measuring equipment faults. It therefore indicates that fixing calibration helps to improve detector performance by 15%, thus the balance of false alarm 22% (37% - 15%) is caused by other sources, namely: distance of detectors from leakage source, extreme condition of working fluid, impact of environment which may be seasonal or periodical on daily bases, and human error.

### 3.3 Major Causes of False Alarm in Geregu Gas Power Plant

#### 3.3.1 False Alarm due to Seasonal Condition of the Plant Environment

According to [46, 47], the central region of Nigeria – particularly the Federal Capital Territory, Abuja, are governed by a well-defined single rainy season (April to September) and dry season (December to March) with October and November as transition period. From this definition, a scatter table for the true and false alarm are shown in Table 3 with '1' in green representing true alarm and '0' in orange indicating false alarm.

Table 3: Scatter plot table for true and false alarm of monthly events per season

Year	Rainy season						Dry season					
	Apr	May	Jun	Jul	Aug	Sep	Oct	Nov	Dec	Jan	Feb	Mar
2019	1			1						0		
2020								1	0	0		
2021										0, 1		
2023		1			1							
2024										0, 0, 1		

As observed in Table 3, the actual gas detector was quite over sensitive (false alarm) in six instances, which is considered appropriate compared to Lin et al., [48] characterization of the detector sensors. From the table, all the instances during which the detector sensor flagged false gas leak alarms (as shown in orange) occurred in December and predominantly in January; during the harmattan periods of each calendar year. This assertion was also confirmed from the records of the Instrumentation and Control unit at Geregu power station, which showed that the false gas detection alarms on those came up on the HMI in the control room due to dusty matter and cobwebs on the lens of the plant gas detectors, and hence, wrong analysis for gas-leakage. This assertion was also aided with further documentation based on detector location. Out of six pairs of detectors deployed within and outside the turbine-built environment, 2 pair were involved in all the given alarms and they were position closer to the outer ambient. Thus, it can be concluded that seasonal and environmental factors are highly responsible for false alarm in the Geregu gas power plant.

### 3.3.2 False Alarm due to Human Factor

Record also indicated that one of the alarms was caused by extreme pressure condition in the combustion chamber. Investigation of this using Y-Y analysis shows that a maintenance schedule was missed in order to meet production target after a previous off-line backwashing that took over 3 hours shutdown. The resultant contributing factors by weight are given in the radar-chart of Figure 6.

From the pentagonal radar graph in Figure 6, the points for both location and thermo-fluid properties fall within the innermost pentagon and are thus considered as having non-substantial effect on the alarm status, [49]. This is followed by the effect of equipment defect which is greatly resolved through calibration processes. The two significant factors that mostly influence false alarm are human error and seasonal conditions. While human error can be managed through staff training on system quality control and assurance management and their impact on safety of human life equipment and environment as well as on productivity. Seasonal factor can be mitigated through planned maintenance policy and reverse engineering via entrance space humidification and use of air curtain among others. These are intended to increase the masses of in-coming dust to change their flow direction towards the ground to make them easily removable.

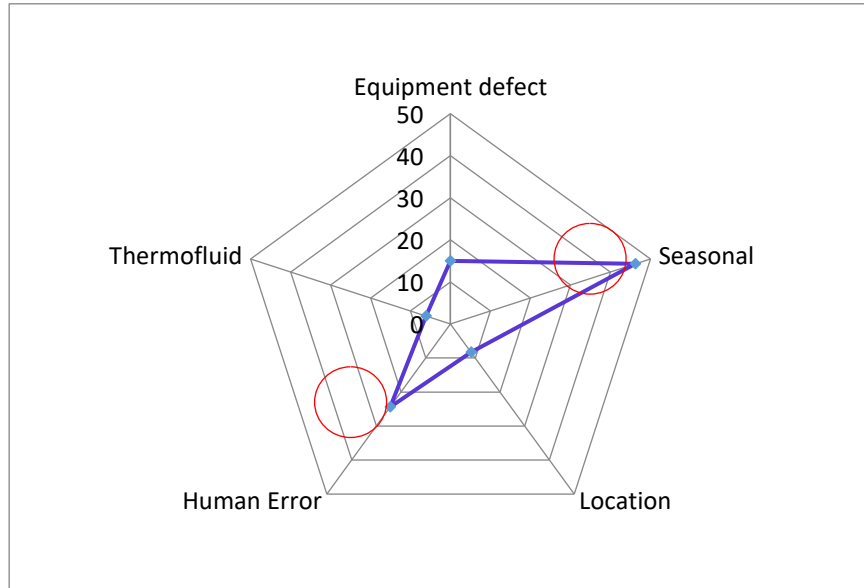


Figure 6: Pentagonal Radar Chart for Gas Leakage Influenced Factors

### 3.4 Performance of Calibrated Detector Integrated with the ANN-model

#### 3.4.1 Model Accuracy

The accuracy of the ANN-integrated calibration model is shown in Table 4 with RMSE and Cross-entropy against the calibrator-target and ANN-integrated model outputs.

Table 4: Gas detector, calibration and ANN Performance Test Samples

Date	Detector (Input)	Calibrator (Target Output)	ANN (Predicted Output)	Root Mean Square Error	Cross - Entropy
02/06/2021	1	1	1	0	0.25238
13/06/2022	1	1	0.9989	0.00000001	0.25076
26/09/2022	1	1	1	0	0.25001
04/10/2022	1	0	0.6753	0.025686473	0.24897
15/02/2024	1	1	0.9358	0.00000729	0.24854
Epoch	r	R <sup>2</sup>	PCG	RMSE	CE
65	0.95	0.87	0.9220	0.3034	0.2501

One of the test samples is presented in Table 4. It covers expected alarm events for three years horizon of calibrated without ANN and calibrated with ANN. The three main measures used are: percentage of good classification (PGC), Root mean square error (RMSE) and cross-entropy (CE). To ascertain the level of relationship between input and output, linear correlation  $r$  and coefficient of determination  $R^2$  were also examined.

After 100 epochs of several training and testing, the optimum training performance using the Levenberg-Marquard technique [50, 51] was taken to be at 65 epochs as shown in Figure 7.

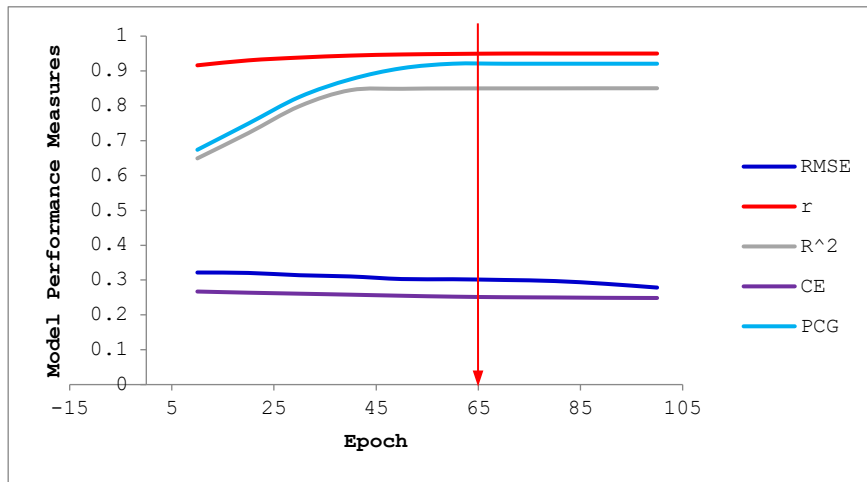


Figure 7: Plot showing best performance measures of the ANN model.

### 3.4.2 Measure of Model Error and Loses

The graphs are classified into two zones; low and high measure value zones. In the low measure value zone are root mean square error (RMSE) and cross-entropy (CE) which are measures of errors and their probability distributions of the predicted and actual values.

From Figure xxx, the average RMSE against 65 Epochs is 0.30 and the cross enthalpy is 0.25. The variation pattern of the RMSE and CE are shown in exploded views of Figure 8.

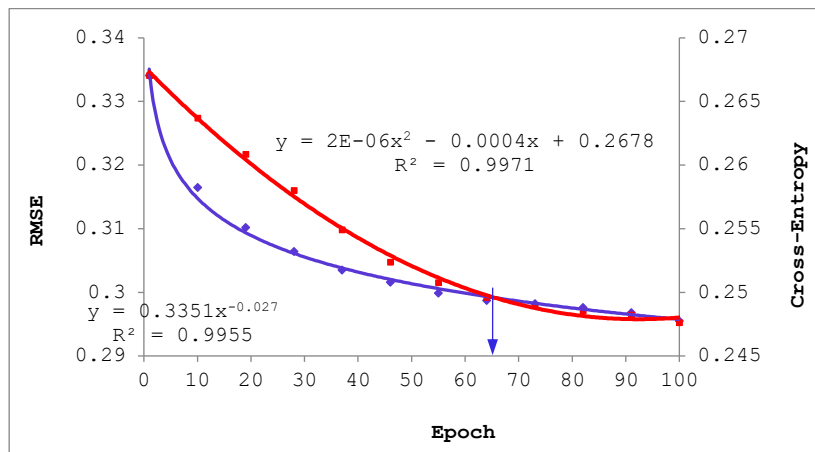


Figure 8: Exploded view of the RMSE and Cross-Entropy

### 3.4.3 Model Correlation and Fitness

At the upper part of the graph 7 are PCG, r and R<sup>2</sup>. The PCG measures the average output of the model and it is seen to have grown quickly to 0.92 at 65 epochs with a linear correlation r of 0.95 and R<sup>2</sup> of 0.87 of the sample data sets as shown in Figure 9

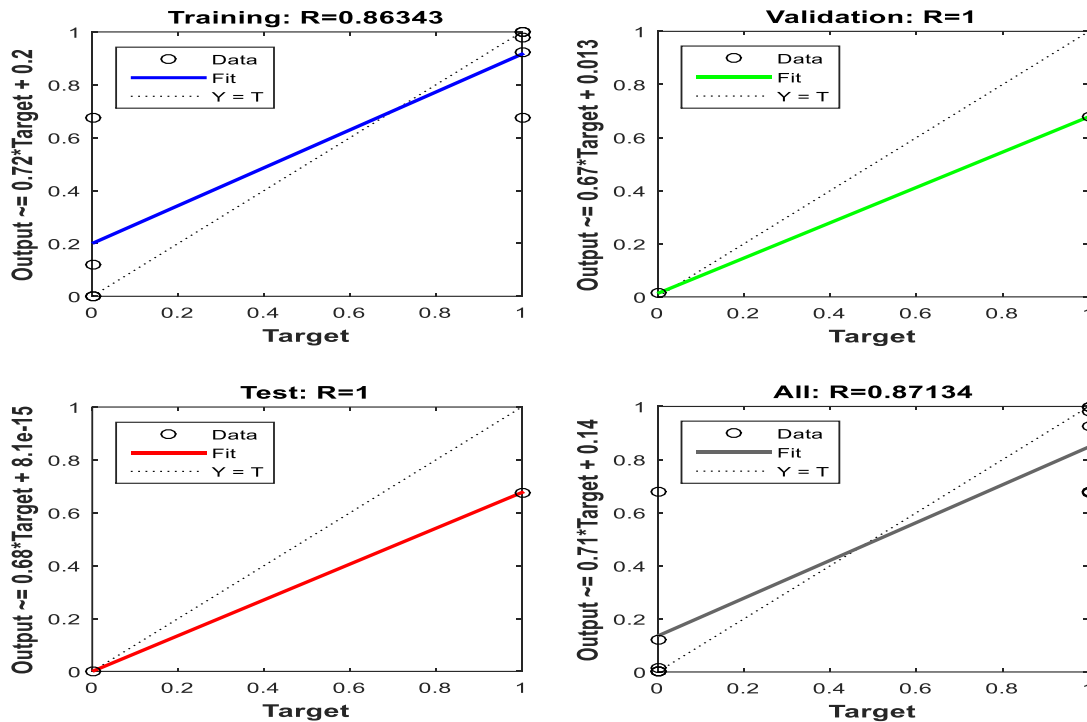


Figure 9: Regression performances for training, validation and test of the ANN model.

The population data shows a more inclusive influence in the determination of variation in the model output with an  $R^2$  of 0.9961 and an  $r$  of 0.98 after data is cleaned of outliers.

The performances of indicate very close correlation between the ANN based detector outputs and the target (calibrator measurements) with large numbers of the data sets influencing the determination of the outputs thus, resulting a high percentage of classification and low RMSE and cross-entropy. The overall results suggest good performance in terms of best fit and accuracy.

#### 4.0 Conclusion

An artificial neural network (ANN) with five input, two hidden layers, and one output based on AND logic gate with binary inputs was developed for true gas leak detection in Geregu power plant. Several factors responsible for gas leak were conventionally summed up around detectors' sensor drifting and thus, calibration process is the only correction measure commonly applied. It was found that even calibrated detectors may still produce false alarm due to seasonal ambient condition, human operation error, extreme pressure imbalances of the working fluid and relative leakage location to fixed detector position. The unique contribution of this study is that it traces the causes of false alarm beyond detectors' sensor drifting to these primary factors expressed in binary representation with AND logic gate to train, validate and test the ANN. The result obtained shows that sensitivity of the actual gas detector is over 170%. While sensor over sensitivity may be reasonable in the short to mid-term life span, it ruins the results in the long run when other factors could have their ways to overcome the sensor weakness due to ageing, thus, leading to false leak detection alarms. As such, it is important to consistently calibrate the detector sensor, which mostly takes a lot of time and operation interruptions. In this study it is seen that a robust and well formulated Artificial Intelligence (AI) based detector sensor model with RMSE of 0.3034 and overall  $R^2$  of 87%, was used to accurately predict gas leakages for true or false scenarios with 92.2% prediction status at an epoch of 65.

It can thus be concluded that an ANN based gas detector sensor can be used to alternatively monitor the sensitivity of the actual gas detector as the model results were validated against calibration data with almost zero differences. Though, the ANN model detectors cannot wholly replace the role of calibration the integration of the two will provide an excellent AI based sensor that will eliminate false alarms and improves productivity in gas power plants.

## References

- [1] Carter S. (2020) Gas leaks-and its worse than we thought. [Online] Available: <https://www.nrdc.org/bio/Sheryl-carter/gas-leaks-and-its-worse-we-thought>.
- [2] Climate Nexus, -Methane at COP27. 2022. <https://climatenexus.org/international/methane-at-cop27>
- [3] Honeywell (2013) gas detection book (vol.5) at <https://www.honeywell.com/>
- [4] Tabuchi H. How Climate Change Deniers Rise to the Top. The New York Times, 2023. <https://www.nytimes.com/2017/12/29/google-search>
- [5] Oloche B., Ozigi I.I., Adeyemi K. and Ikpe E. Construction and Leakage Detection of a Dome-Type Biogas Digester in a Village at Abuja, Nigeria. **UOYE Journal of Engineering and Technology**, 2017; 2(1). DOI:10.46792/fuoyejt.v2i1.63
- [6] Nicol R. Fire and gas mitigation after protection fails. Sage Journals, (2006); Vol 39/10 D. <https://journals.sagepub.com/doi/pdf>
- [7] Ghandhi M., Rowley J., Nelson D. and Campbell C. Gas detection in process industry- The practical Approach. Institution of Engineers, 2015, Series 160. <https://www.icheme.org/media/xxv-poster-07.pdf.poster>
- [8] Hangeui Sensors. An in-depth Look at Gas Detection in Power Plant. Hangeui, 2023. <https://www.hangweisensors.com/knowledge/gas-ddetection-in-powerplants/>
- [9] CO<sub>2</sub> meter.com -Industrial and Fixed Gas Detectors; Types and Uses. (2024, April 23). <https://www.CO2meter.com/blogs/news/what-is-an-industrial-fixed-gas-detector#>
- [10] Muda R. Wikipedia, 2009. [https://en.wikipedia.org/wiki/gas\\_detector](https://en.wikipedia.org/wiki/gas_detector)
- [11] Emerson Automation Experts: Gas detection in power generation. (September 8, 2013). <https://www.emerson.com/en-us/common-applications/gas-detection-in-power-generation>
- [12] Gas Detectors NZ. Gas Detection for Power Stations. <https://www.gasdetectors.co.nz/gas-detection-applications/gas-detection-power-stations/>.
- [13] Sensidyne Limited. Power Plant Gas Detection. <https://sensidyne.com/Application/power-plant-detection/>
- [14] Enroth P. and Crosley B. Reducing Risk at Compressor Stations Through Gas and flame detection. Pipeline and gas journal, 2019. <https://www.det-tronics.com/Documents/Det-reducing-risks-at-compressor-stations-ar-1137.pdf>.
- [15] Dräger Limited - Gas Turbines. (ND). [https://www.draeger.com/Documents/Content/gas\\_turbines-note-pdf-10220-en-us-2005-1.pdf](https://www.draeger.com/Documents/Content/gas_turbines-note-pdf-10220-en-us-2005-1.pdf).
- [16] Cepa J. J., Pavón R. M., Caramés P. and Alberti, M. G. A Review of Gas Measurement Practices and Sensors for Tunnels. Sensors National Institutes of Health (NIH), Basel, 2023; 23(3): doi:10.3390/s23031090. <https://www.ncbi.nlm.nih.gov/articles/PMC9919948>
- [18] Faramarz H. B. and Vahid G. Compensation for the drift-like terms caused by environmental fluctuations in the responses of chemo resistive gas sensors. Journal of Sensors and Actuators B Chemical, 2010; 143(2):641-648. DOI:10.1016/j.snb.2009.10.006
- [19] Kendler S. and Zuck A. The Challenges of Prolonged Gas Sensing in the Modern Urban Environment, Journal of Sensors, Basel, 2020; 20(18): 51 - 89. doi: 10.3390/s20185189
- [20] Marko K., Haith A. M. & Harran M. Sensitivity to prediction error in reach adaptation. Journal of Neurophysiol, 2012; 108(6):1752-1763. DOI:10.1152/jn.1001777.2012 <https://www.researchgate.net/228>
- [21] Benammar M., Ahmad S. H. M., Abdaoui A., Tariq H., Touati F., Al-Hitmi A. M. and Crescini, D. A smart rig for calibration of gas sensor nodes. Sensors, 2020; 20(8); 23-41. doi.10.3390/s0082341
- [22] Kwon Y. M., Oh B., Purbia R., Chae H. Y. Han G. H. Kim S.W., Choi K. J., Lee Y., Kim J. J. and Baik M. J. High performance and self-calibrating multi-gas species with sub ppm level. Sensors and actuators B: Chemical, 2023; vol.375, <https://doi.org/10.1016/j.snb.2022.132939>
- [23] Martek Marine. How often should Gas Detectors be Calibrated? <https://www.martek-marine.com/calibrated-frequency-gas-detectors/portable/calibrated-frequency/>



- [46] A., Hommel G. and Blettner M. Linear Regression Analysis. Pub Med central journal, Dtsch Arztebl Int., 2010; [Doi:10.3238/arztebl.2010.0776](https://doi.org/10.3238/arztebl.2010.0776).
- [47] World Bank. Climate Change Knowledge Portal, 2021. <https://climateknowledgeportal.worldbank.org>
- [47] Anyashola A. M., Jacob S. O. and Salami A. W. Evaluation of impact of climate change and urbanization on the water supply of Abuja, Nigeria. International journal of sustainable development, 2015; vol. 17(17). <https://www.researchgate.net/publication/30183324>
- [49] Lin M. F., Cheng C., Yang C. C., Hsiao W. T. and Yang C. R. A wearable and highly sensitive capacitive pressure sensor integrated a dual-layer dielectric layer of PDMS microcylinder array and PVDF electrospun fiber. Organic Electronics Journal, 2021; 98(22):106290. <https://doi.org/10.1016/j.orgel.2021.106290>
- [50] Le Xi., Yadong L. V., Feng J. and Yanyan H. Synthesis of UV-resistant and colourless polyimide films for optoelectrical applications. NPJ - Materials Degradation, 2024; 8(1). DOI:10.1038/s41529-023-00422-w
- [51] Lamamra K. and Rechem D. Artificial neural network modelling of a gas sensor for liquefied petroleum gas detection. Conference: 2016 8th International Conference on Modelling, Identification and Control (ICMIC). DOI:10.1109/ICMIC.2016.7804292
- [52] Shah Z., Raja M. A. Z., Khan W. A., Shoaib M., Asghar Z., Waqas, M. and Muhammad T. Application of Levenberg–Marquardt technique for electrical conducting fluid subjected to variable viscosity. Indian journal of physics, (2022) ; vol. 96 :3901-3919 <https://link.springer.com/article/10.1007/s12648-022-02307-1>